The Astrophysical Journal Letters, 946:L31 (14pp), 2023 March 20 https://doi.org/10.3847/2041-8213/acc39c
© 2023. The Author(s). Published by the American Astronomical Society.
OPEN ACCESS

GRB 221009A: The BOAT

Eric Burns[1], Dmitry Svinkin[2], Edward Fenimore[3], D. Alexander Kann[4], José Feliciano Agüí Fernández[5], Dmitry Frederiks[2], Rachel Hamburg[6], Stephen Lesage[7,8], Yuri Temiraev[2], Anastasia Tsvetkova[2,9], Elisabetta Bissaldi[10,11], Michael S. Briggs[7,8], Sarah Dalessi[7,8], Rachel Dunwoody[12], Cori Fletcher[13], Adam Goldstein[13], C. Michelle Hui[14], Boyan A. Hristov[8], Daniel Kocevski[14], Alexandra L. Lysenko[2], Bagrat Mailyan[15], Joseph Mangan[16], Sheila McBreen[12], Judith Racusin[17], Anna Ridnaia[2], Oliver J. Roberts[13], Mikhail Ulanov[2], Peter Veres[7,8], Colleen A. Wilson-Hodge[14], and Joshua Wood[14]
[1] Department of Physics and Astronomy, Louisiana State University, Baton Rouge, LA 70803 USA; ericburns@lsu.edu
[2] Ioffe Institute, 26 Politekhnicheskaya, St. Petersburg, 194021, Russia
[3] Los Alamos National Laboratory, P.O. Box 1663, Los Alamos, NM 87545, USA
[4] Hessian Research Cluster ELEMENTS, Giersch Science Center, Max-von-Laue-Straße 12, Goethe University Frankfurt, Campus Riedberg, D-60438 Frankfurt am Main, Germany
[5] Instituto de Astrofísica de Andalucía (IAA-CSIC), Glorieta de la Astronomía s/n, E-18008 Granada, Spain
[6] Université Paris-Saclay, CNRS/IN2P3, IJCLab, F-91405 Orsay, France
[7] Department of Space Science, University of Alabama in Huntsville, 320 Sparkman Drive, Huntsville, AL 35899, USA
[8] Center for Space Plasma and Aeronomic Research, University of Alabama in Huntsville, Huntsville, AL 35899, USA
[9] Dipartimento di Fisica, Università degli Studi di Cagliari, SP Monserrato-Sestu, km 0.7, I-09042 Monserrato, Italy
[10] Dipartimento Interateneo di Fisica, Politecnico di Bari, Bari, Italy
[11] Istituto Nazionale di Fisica Nucleare, Sezione di Bari, Bari, Italy
[12] School of Physics, Centre for Space Research, Science Center North, University College Dublin, Dublin 4, Ireland
[13] Science and Technology Institute, Universities Space and Research Association, 320 Sparkman Drive, Huntsville, AL 35805, USA
[14] ST12 Astrophysics Branch, NASA Marshall Space Flight Center, Huntsville, AL 35812, USA
[15] Department of Aerospace, Physics and Space Sciences, Florida Institute of Technology, Melbourne, FL 32901, USA
[16] Laboratoire de Physique des 2 infinis Irène Joliot-Curie—IJCLab, CNRS / Université Paris-Saclay / Université Paris Cité, Bâtiment 104 Rue Henri Becquerel, F-91405 Orsay Campus, France
[17] NASA Goddard Space Flight Center, Greenbelt, MD 20771, USA
Received 2023 February 27; revised 2023 March 11; accepted 2023 March 13; published 2023 March 28

Abstract

GRB 221009A has been referred to as the brightest of all time (BOAT). We investigate the veracity of this statement by comparing it with a half century of prompt gamma-ray burst observations. This burst is the brightest ever detected by the measures of peak flux and fluence. Unexpectedly, GRB 221009A has the highest isotropic-equivalent total energy ever identified, while the peak luminosity is at the ∼99th percentile of the known distribution. We explore how such a burst can be powered and discuss potential implications for ultralong and high-redshift gamma-ray bursts. By geometric extrapolation of the total fluence and peak flux distributions, GRB 221009A appears to be a once-in-10,000-year event. Thus, it is almost certainly not the BOAT over all of cosmic history; it may be the brightest gamma-ray burst since human civilization began.

Unified Astronomy Thesaurus concepts: Gamma-ray bursts (629); Gamma-ray transient sources (1853); Gamma-ray sources (633); Jets (870); Core-collapse supernovae (304)

1. Introduction

Cosmological gamma-ray bursts (GRBs) are the most luminous electromagnetic events identified in the universe since the big bang. GRBs were accidentally discovered in 1967 by the Vela series of satellites launched to monitor Earth for atmospheric nuclear detonation signatures following the Partial Nuclear Test Ban Treaty (Klebesadel et al. 1973). Through Vela, its successors, and instruments designed for astrophysics and planetary research, humanity has monitored the full gamma-ray sky for 55 yr.

Cosmological GRBs arise from bipolar, relativistic jets powered by compact central engines (Zhang 2018). These jets undergo internal dissipation releasing the prompt GRB emission in the keV and MeV regimes and subsequently interact with the circumburst material to develop an external shock that releases synchrotron emission across the electromagnetic spectrum, referred to as afterglow. Cosmological GRBs are separated into two overlapping classes based on prompt duration, generally separated by a threshold value of 2 s (Mazets et al. 1981; Dezalay et al. 1991; Kouveliotou et al. 1993), which are now known to have different progenitor systems. Short GRBs arise from neutron star mergers (Abbott et al. 2017; Goldstein et al. 2017; Savchenko et al. 2017); long GRBs arise from collapsars, a rare, fast-rotating subset of core-collapse supernovae (Galama et al. 1998; Cano et al. 2017).[18] A small number of detected short GRBs are magnetar giant flares (Mazets et al. 1979, 2008; Burns et al. 2021; Svinkin et al. 2021), which are not of interest here since they have a distinct physical origin.

Original content from this work may be used under the terms of the Creative Commons Attribution 4.0 licence. Any further distribution of this work must maintain attribution to the author(s) and the title of the work, journal citation and DOI.

[18] Notably, some GRBs have contradicted the 2 s divide. Recent exemplars include the temporally short supernova-associated GRB 200826A (Ahumada et al. 2021; Zhang et al. 2021; Rossi et al. 2022b) and the temporally long, nearby kilonova-associated (i.e., strongly suggestive of a neutron star merger origin) GRB 211211A (Rastinejad et al. 2022; Troja et al. 2022; Gompertz et al. 2023).

Table 1
Basic Properties and 4π yr Equivalent Coverage for GRB Monitors Whose Data Were Studied in Detail for This Catalog

Instrument	Vela	PVO	BATSE	Konus-Wind	Fermi-GBM
Start date	690703	780914	910421	941112	080714
End date	730610	921004	000513	230307*	230307*
Calendar observing years	3.9	13.3	9.7	28.3	14.6
All-sky observing fraction	100%	100%	67%	100%	70%
Live-time fraction	100%	90%	73%	90%	85%
4π yr equivalent coverage	3.9	11.9	4.7	25.5	8.8
Fluence reporting range (keV)	300–1500	100–2000	20–2000	20–10,000	10–1000
Peak flux interval (s)		0.250	2.048	0.064	1.024
GRB sample size	20	318	2704	∼3500	∼3500

Note. The BATSE observing fraction is determined from orbital height and live time inferred from Hakkila et al. (2003). Vela is assumed to have 100% coverage. Other values are taken from the cited references for each instrument. Note that the end dates for Konus and GBM refer to the end of our sample, as do the total number of GRBs; both are still observing at the time of publication.

The brightness of prompt GRBs can be quantified through different parameters. The time-integrated brightness at Earth is the fluence, which corresponds to the intrinsic brightness measure $E_{\rm iso}$, the total isotropic-equivalent energetics calculated by assuming an equal fluence over a sphere centered on the source with a radius equal to the luminosity distance from source to Earth (Piran 1999). The peak flux corresponds to the highest time-resolved flux in a specified interval of time as measured at Earth, with $L_{\rm iso}$ being the isotropic-equivalent measure of the maximum power output in a specified interval. When the opening angle of the jetted outflow is known, the isotropic-equivalent energetics can be converted to the more accurate collimation-corrected energetics (Sari et al. 1999).

The exceptionally bright long GRB 221009A was discovered by a fleet of satellites on 2022 October 9 (e.g., Gotz et al. 2022; Kozyrev et al. 2022; Lapshov et al. 2022; Liu et al. 2022; Piano et al. 2022; Ursi et al. 2022; Xiao et al. 2022; An et al. 2023; Frederiks et al. 2023; S. Lesage et al. 2023, in preparation; Ripa et al. 2023; Williams et al. 2023), as well as particle detectors on board MAVEN, GAIA, STEREO (R. Leske 2023, private communication), ACE (R. Leske 2023, private communication), and Voyager 1 (A. Cummings 2023, private communication; the detection by Voyager 1, however, occurred on the 8th). The GRB has been observed across the electromagnetic spectrum, from beyond 10 TeV by LHAASO (Huang et al. 2022) down to radio (e.g., Fulton et al. 2023; Kann et al. 2023; Laskar et al. 2023; Malesani et al. 2023; O'Connor et al. 2023; Tiengo et al. 2023; Williams et al. 2023). Other key observations include the first observations of the prompt and afterglow polarization from the same burst (Negro et al. 2023), the (somewhat) surprising (Murase et al. 2022) lack of neutrinos (Abbasi et al. 2023), and the first disruptive target of opportunity from an out-of-cycle proposal of JWST (Levan et al. 2023; also the first JWST observation of a GRB afterglow ever).

GRB 221009A was initially flagged as having the highest prompt fluence and peak flux ever identified by both the Fermi Gamma-ray Burst Monitor (GBM) and the Konus-Wind (Konus) instruments (Frederiks et al. 2022; Veres et al. 2022). As each instrument has individually identified ∼3500 GRBs, constituting the two largest prompt GRB samples, GRB 221009A was referred to as the brightest of all time (BOAT). Given the age and size of the universe, it is exceedingly unlikely that GRB 221009A is truly the brightest ever. Colloquially, this statement refers to the brightest prompt phase from identified GRBs.

This paper quantifies the validity of the BOAT claim for prompt emission by comparing the Konus and GBM observations of GRB 221009A with the broader sample of (nearly) all prompt GRBs identified since their discovery. The Fermi-GBM paper (S. Lesage et al. 2023, in preparation) and the Konus-Wind paper (Frederiks et al. 2023) focus on the respective analyses of this burst and place it into context of the respective samples. We refer the reader to both papers for those details. This paper makes use of the analyses in both papers and is intended to be complementary. Our sample compilation and input catalogs are explained in Section 2. The bright samples for fluence, peak flux, $E_{\rm iso}$, and $L_{\rm iso}$ are presented in Section 3. The immediate implications of our work are explored in Section 4, and we provide conclusions in Section 5.

2. Sample

Numerous GRB monitors have been launched to study these events (Tsvetkova et al. 2022). The monitors of focus for this work and key metrics are given in Table 1. For bright bursts, observed spacetime volume can be represented as a continuous full-sky equivalent value, i.e., number of 4π yr. The maximal value is ∼55, from the discovery of the first GRB in 1967 until the end of our sample on 2023 March 7; however, not all data are publicly available. Notable gaps in coverage occur from the discovery of GRBs in 1967 until the start of our Vela sample and from the end of our Vela sample until the launch of Pioneer Venus Orbiter (PVO), limiting the available maximal value to ∼48. Altogether, our data from Vela, PVO, the Burst And Transient Source Experiment (BATSE), Konus-Wind, and Fermi-GBM provide a 4π yr equivalent coverage of 44.3 yr, which is ∼92% of the possible public total. An additional literature search, described below, has increased this fraction. We thus expect our fluence and peak flux coverage to be largely complete.

While not utilized to construct our GRB sample, we highlight the importance of the Neil Gehrels Swift Observatory (hereafter Swift) for this work (Gehrels et al. 2004). Its arcminute-scale localizations by the Burst Alert Telescope (BAT; Barthelmy et al. 2005) prompt follow-up with the narrow-field instruments XRT and UVOT (Burrows et al. 2005; Roming et al. 2005), and immediate reporting to the follow-up community has been critical for construction of the redshift sample of GRBs. For bursts with reported redshift and broadband spectral observations, Swift localizations with

Konus-Wind and Fermi-GBM spectral coverage provide the vast majority of the total sample.

2.1. Input Sample

While GRBs were discovered in 1967, quantitative study of their brightness began with GRB 690703, the first GRB observed with the Vela 5A and 5B satellite pair launched in May of that year. Our Vela sample begins with that burst and ends in 1973, the last year with publicly reported data. Fluence values are taken from Strong et al. (1974); peak flux measurements are not available. PVO observed for 14 yr with all-sky coverage and high live time (Klebesadel et al. 1980; Fenimore et al. 1993b), covering a quarter of the total possible 4π yr sample. The PVO fluence and peak flux values are taken from Fenimore et al. (2023), which is an updated version using additional checks from the data presented in Fenimore et al. (1993a). The most sensitive GRB monitor ever flown is CGRO-BATSE. The BATSE fluence and peak flux values are compiled in the 5B Spectral Catalog (Goldstein et al. 2013), available on HEASARC.[19]

With nearly 28 yr of full-sky observing with high live time, Konus-Wind (Aptekar et al. 1995) alone covers more than half of the total sample of bright bursts. A search for the highest fluence and peak flux bursts in the Konus sample was performed for this work and is expected to be complete in fluence down to a few $\times 10^{-4}$ erg cm^{-2}. The $E_{\rm iso}$ and $L_{\rm iso}$ samples for Konus are compiled in two publications (Tsvetkova et al. 2017, 2021) with updates through March 2023 for this work.

Our last considered instrument is the Fermi-GBM. The 4π yr equivalent coverage of GBM is limited by the particle activity and Earth blockage of the sky inherent to a low Earth orbit (which also affects BATSE). The GBM observations are additionally critical for proper use of the full Vela, PVO, and BATSE GRB samples. GBM has the widest energy coverage of any GRB monitor, and the GBM 10 Year Spectral Catalog (Poolakkil et al. 2021) is complete with respect to the onboard trigger catalog (von Kienlin et al. 2020), both of which are available on HEASARC.[20] These together allow for the standardization of fluence and peak flux measurements in our various input instruments, described in the next section.

Lastly, to capture all identified bright bursts, we utilized GRBCAT[21] and the BeppoSAX GRB Spectral Catalog (Guidorzi et al. 2011), as well as a search for known or forgotten bright bursts in NASA ADS, and for recent bright bursts reported in publications or initial results in GCN circulars. All bright Konus-Venera GRBs reported (Mazets et al. 1981) are contained in the PVO catalog. It is feasible that some bright bursts escaped our searches. Notably, there is no reported GRB catalog from GINGA. However, with the Vela satellites and successors we are confident that any burst of sufficient brightness that may affect our conclusions would certainly be known, and we are confident in the claims that follow.

2.2. Standardizing the Sample

Due to different instrument designs and analysis decisions, our input catalogs report brightness measurements integrated over different energy ranges. Comparison between instruments requires conversion to a uniform energy range. In order to account for nearly all emission, we set this uniform energy range to the standard bolometric range of 1 keV–10 MeV (e.g., Racusin et al. 2009; Tsvetkova et al. 2017). For intrinsic measures these values are k-corrected (Bloom et al. 2001). Although this will miss significant high-energy emission in a small subset of bursts (see Agüí Fernández et al. 2023, for an application of an even broader energy range), it is better matched to the observing range of all considered instruments.

For Konus-Wind we utilize the standard reported values of 20 keV–10 MeV for fluence and peak flux, which are sufficiently close to bolometric values, and the catalog-reported k-corrected 1 keV–10 MeV values for $E_{\rm iso}$ and $L_{\rm iso}$ (Tsvetkova et al. 2017). For all other instruments, we convert measurements to the bolometric energy band of 1 keV–10 MeV; for intrinsic measures this is defined in the rest frame and accounts for cosmological k-correction. For GBM and BATSE bursts best fit by spectra with curvature (as determined through the standard catalog methods; Goldstein et al. 2013; Poolakkil et al. 2021) we directly calculate bolometric energetics by sampling parameter value distributions for proper, asymmetric error propagation.

For PVO and Vela bursts we cannot directly calculate bolometric energetics. For GBM and BATSE bursts best fit by a power law we cannot accurately extrapolate to bolometric brightness owing to a lack of determination of spectral curvature. For each instrument, we utilize the GBM sample (Poolakkil et al. 2021) to determine the scaling distribution from the initial energy range to the bolometric energy range. This is determined separately for peak flux and fluence, due to the different hardness in peak intervals verse time-integrated spectra. PVO values are scaled from the 50–300 keV peak flux and fluence values, as they were determined using the modern Band function (Band et al. 1993). For determining the scaling distributions to apply to Vela, we exclude GBM bursts with $E_{\rm peak}$ less than 300 keV, as similar bursts are unlikely to trigger the Vela instruments owing to the higher low-energy threshold. Further details of this procedure are described in Appendix B.

Given the sharply peaked pulse structure of GRBs, shorter peak flux intervals will correlate with high inferred peak flux values. In Appendix B we show that peak flux values will increase by ∼15% for each step of two toward shorter intervals. For all $L_{\rm iso}$ measures we have converted the native 0.064 s interval for Konus, 0.250 s interval for PVO, and 2.048 s interval for BATSE to the 1.024 s interval for GBM, matching the measured timescale for GRB 221009A. An inversion of this procedure is used for log$N$–log$P$ comparisons in Section 4.1.

Uncertainties are fully calculated throughout this paper. For $E_{\rm iso}$ and $L_{\rm iso}$ the typical 1σ fractional uncertainty is $\lesssim$10%. For fluence and peak flux the corresponding numbers are 35% and 45%, respectively, which are larger owing to the application of our scaling methods to some bursts (detailed in Appendices A and B), which are only rarely necessary for the isotropic-equivalent energetics calculations. The uncertainties do not affect any of our conclusions and are therefore omitted for brevity.

To check intercalibration uncertainty between instruments, fluence was compared for bursts seen by two instruments, showing average overall agreement within ∼20%. Additional confirmation that this approach is reasonable is given by the log$N$–log$S$ agreement in the next section. To match the sample

[19] https://heasarc.gsfc.nasa.gov/W3Browse/cgro/bat5bgrbsp.html
[20] https://heasarc.gsfc.nasa.gov/W3Browse/fermi/fermigtrig.html
[21] https://heasarc.gsfc.nasa.gov/grbcat/

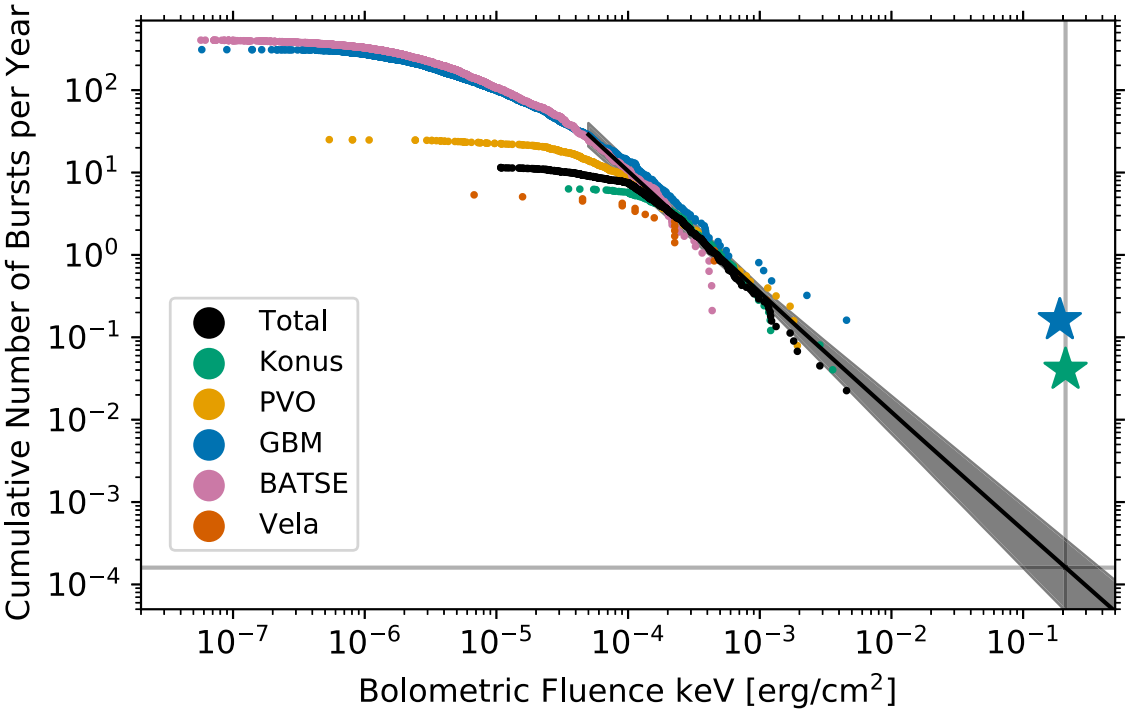

Figure 1. Points indicate the annualized log$N$–log$S$ distributions for GBM, PVO, BATSE, Konus, and Vela. A merged total sample is presented with a fit (from Section 4.1) to the combined log$N$–log$S$ distribution with index measured as -1.47 ± 0.15 (90% confidence interval). GRB 221009A stands alone, with the Konus and GBM measurements of this burst denoted by stars. A vertical line maps the observed fluence of GRB 221009A to the power-law extrapolation, and the horizontal line marks the inverse recurrence rate of events this bright.

to the long GRB class of GRB 221009A, we exclude bursts that are obviously of the cosmological short class (durations under 2 s). We additionally exclude bursts that are known to be magnetar giant flares, as they originate from a distinct physical origin. Thus, the samples below should be mostly composed of long GRBs arising from collapsars. For the intrinsic energetic figures, some short bursts are shown for comparison.

3. GRB 221009A in Context

Peak flux and fluence values for GRB 221009A are taken from Konus (Frederiks et al. 2023) and GBM (S. Lesage et al. 2023, in preparation). Both observations are nonstandard, given the unprecedented brightness of this event. The Konus and GBM teams worked in isolation before comparing values, allowing for independent checks on reconstruction accuracy. We additionally compare with the brightness measures from INSIGHT-HXMT and GECAM-C, reported in An et al. (2023). The GBM numbers presented here are preliminary; however, due to general agreement with other values of the brightness of prompt emission of GRB 221009A, the values are suitably robust for our purposes here. For intrinsic energetics we use the redshift of 0.151 (de Ugarte Postigo et al. 2022; Malesani et al. 2023) and a typical cosmology[22] giving a luminosity distance of 724 Mpc. When a given burst is identified by more than one facility, we use the highest brightness value reported.

While this paper was under review, GRB 230307A was detected by GBM, Konus, and other instruments (Dalessi et al. 2023; Svinkin et al. 2023). With the initial results this burst has the second-highest energy fluence ever reported. The initial results for this burst are included for the fluence and peak flux discussions below, but not in the intrinsic energetics section (as a redshift is currently not known).

3.1. Fluence

The fluence S of GRB 221009A is 0.21 ± 0.02 erg cm^{-2} as measured by Konus-Wind (Frederiks et al. 2023) and $\sim$0.19 erg cm^{-2} as measured by Fermi-GBM (S. Lesage et al. 2023, in preparation). These values are in agreement with the INSIGHT-HXMT and GECAM-C bolometric fluence of 0.224 ± 0.002 (An et al. 2023). log$N$–log$S$ is the cumulative number of events N above a given fluence S; GRB 221009A is compared against our annualized log$N$–log$S$ distributions from our considered instruments in Figure 1. Our samples of interest show broad agreement, noting the significant uncertainty due to low counts at particularly high fluence. In this regime, truncation due to instrumental limitations may also be significant.

Table 2 contains the brightest bursts in our sample, including bursts from additional instruments beyond those considered in our main sample. Of the 15 other bursts with a bolometric fluence in excess of 10^{-3} erg s^{-1} cm^{-2}, only 2 have durations comparable to or longer than GRB 221009A.

3.2. Peak Flux

For GRB 221009A the peak flux P measured over a 1 s timescale by Konus-Wind is 0.031 ± 0.005 erg s^{-1} cm^{-2}, with temporal precision limited by the return to lower-resolution data. The preliminary 1.024 s peak flux as measured by Fermi-GBM of this burst is 0.01 erg s^{-1} cm^{-2}. The INSIGHT-HXMT and GECAM-C 1 s peak flux value of 0.0172 ± 0.0003 is consistent (An et al. 2023). We follow our procedure of using the highest reported value for a given measure. These values

[22] That is, the default flat universe with $H_0 = 69.6$ and $\Omega_m = 0.286$ from https://astro.ucla.edu/~wright/CosmoCalc.html.

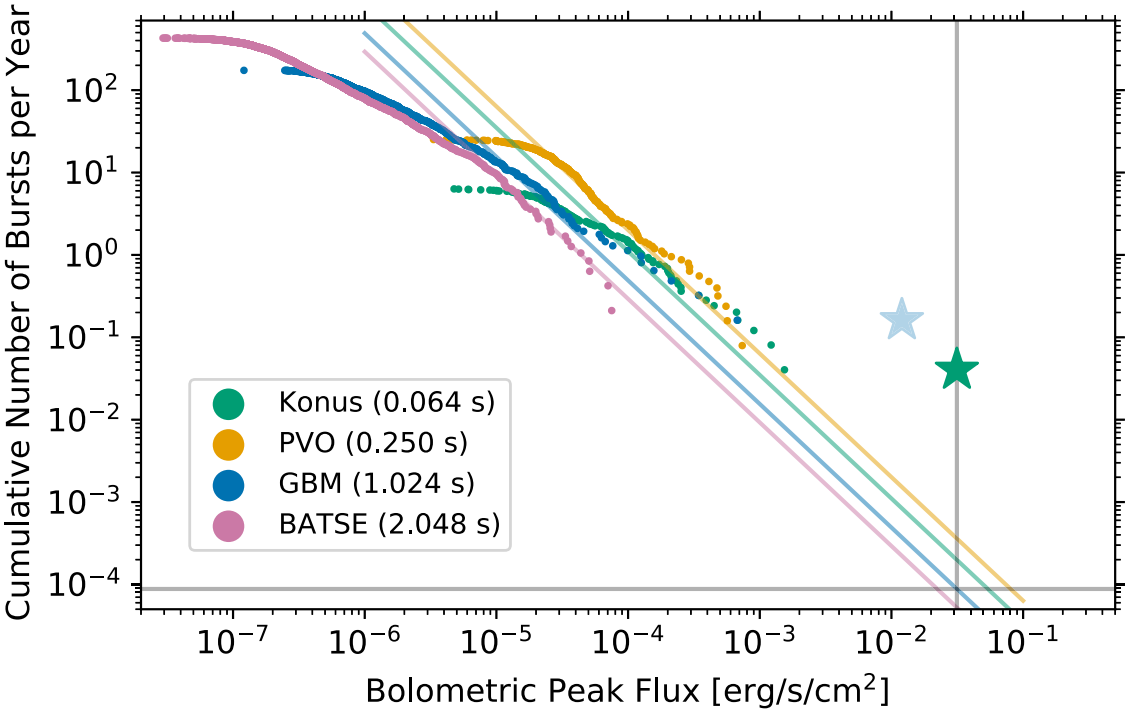

Figure 2. Points indicate the annualized log$N$–log$P$ distributions for GBM, PVO, BATSE, and Konus, with peak flux interval indicated in the legend. A power law with fixed index of $-3/2$ is shown for each separate burst sample. The GBM and BATSE distributions are fit above 1×10^{-5} erg s^{-1} cm^{-2}; the Konus and PVO distributions are fit above 5×10^{-5} erg s^{-1} cm^{-2}. GRB 221009A measures are shown with stars, and again it is a significant outlier. The GBM measure of GRB 221009A is faded to indicate that it may be an underestimate.

Table 2
GRBs with Fluence $>10^{-3}$ erg s^{-1} cm^{-2}

GRB Name	Duration (s)	Fluence (erg cm^{-2})	Energy Range (keV)	Instrument	Reference
GRB 221009A	600	0.21	1–10,000	Konus, GBM	Frederiks et al. (2023), S. Lesage et al. (2023, in preparation)
GRB 230307A	200	4.56×10^{-3}	1–10,000	GBM, Konus	Dalessi et al. (2023), Svinkin et al. (2023)
GRB 130427A	62	2.86×10^{-3}	20–10,000	Konus, GBM	Tsvetkova et al. (2017), Poolakkil et al. (2021)
GRB 840304	1000	$\sim 2.8 \times 10^{-3}$	1–10,000	PVO	Klebesadel et al. (1984), Chuang (1990)
GRB 830801	30	$>2.00 \times 10^{-3}$	30–7500	SIGNE 2 MP9	Kuznetsov et al. (1987)
GRB 920212	14	1.93×10^{-3}	1–10,000	PVO	Fenimore et al. (2023), This work
GRB 900808	7.2	1.81×10^{-3}	1–10,000	PVO	Fenimore et al. (2023), This work
GRB 940703A	31.4	1.60×10^{-3}	100–10,000	PHEBUS-GRANAT	Barat et al. (1998)
GRB 811016	13.2	1.33×10^{-3}	1–10,000	PVO	Fenimore et al. (2023), This work
GRB 160625B	680	1.23×10^{-3}	1–10,000	GBM, Konus	Poolakkil et al. (2021), This work
GRB 180914B	150	1.21×10^{-3}	20–10,000	Konus	Frederiks et al. (2018)
GRB 140219A	18	1.20×10^{-3}	20–10,000	Konus	Golenetskii et al. (2014)
GRB 160821A	47	1.17×10^{-3}	20–10,000	Konus, GBM	Kozlova et al. (2016), Poolakkil et al. (2021)
GRB 911027	111	1.15×10^{-3}	1–10,000	PVO	Fenimore et al. (2023), This work
GRB 710630	~ 7	1.13×10^{-3}	1–10,000	Vela	Strong et al. (1974), This work
GRB 910402	35.9	1.11×10^{-3}	100–10,000	PHEBUS-GRANAT	Barat et al. (1998)
GRB 021206	5.2	1.08×10^{-3}	20–10,000	Konus	This Work

Note. The brightest measurements for a given burst are reported. GRB 940703A and GRB 910402 were identified by BATSE, but we use the higher values reported by PHEBUS-GRANAT measures for the same bursts. GRB 830801, perhaps the third-highest fluence ever, was measured by SIGNE 2 MP9. The value for GRB 840304 is taken from the dedicated analysis on this burst. References contain more details on individual bursts. Durations here are not a uniformly measured quantity (estimated from light curve, T_{90}, T_{100}) and are only intended to be approximate.

are compared against the annual log$N$–log$P$ distributions from our instruments in Figure 2.

The peak flux of GRB 221009A is most directly compared with the GBM values, given the 1.024 s peak interval. As expected, the 2.048 s peak flux distribution from BATSE has systematically lower values than the 1.024 s distribution from GBM, which is lower than the 0.064 s distribution from Konus. With proper selection of considered events and analysis of BATSE data not available in the BATSE catalogs, the PVO and BATSE log$N$–log$P$ distributions show strong agreement (Fenimore et al. 1993a); however, our 0.250 s PVO distribution is anomalously high. The origin of this is not well understood

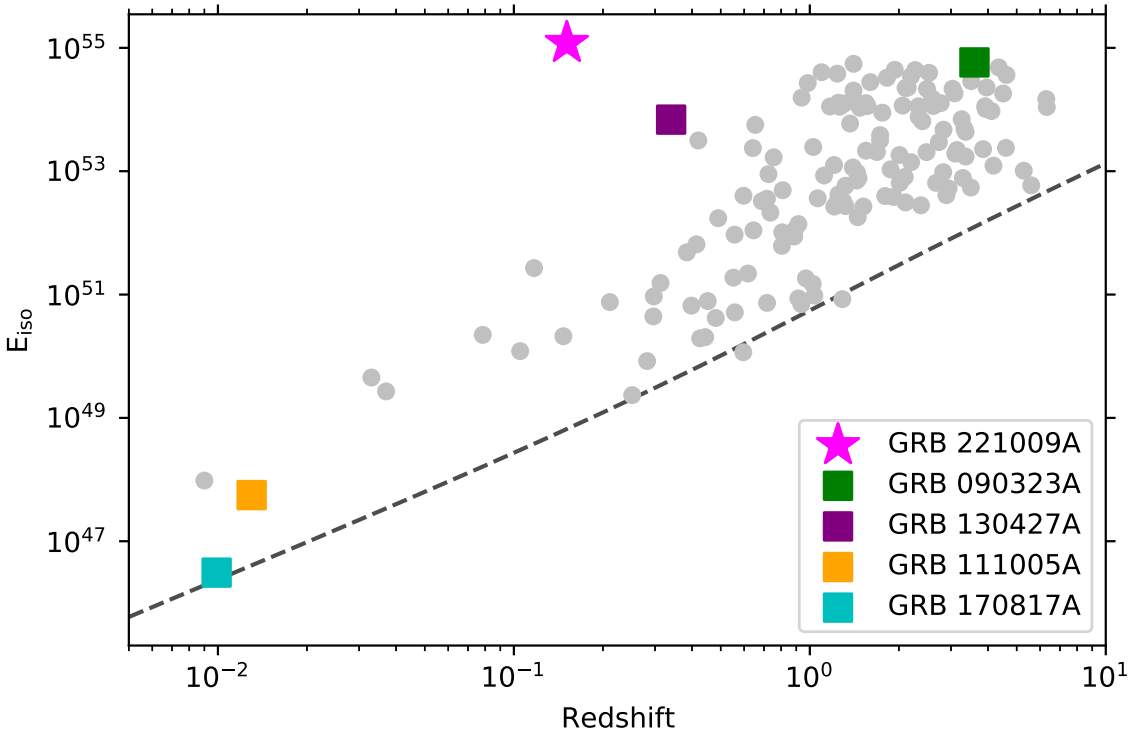

Figure 3. Bolometric, *k*-corrected E_{iso} for nearly 150 GRBs compiled from the literature (Abbott et al. 2017; Tsvetkova et al. 2017), with additional bright and faint GRBs compiled following those works and for future analyses. The dashed line is an approximate, empirical detection threshold for GRBs as a function of redshift. Extreme GRBs are highlighted: GRB 130427A, the previous fluence record holder; GRB 090323A, the previous E_{iso} record holder; GRB 111005A, the lowest known E_{iso} for a collapsar; and GRB 170817A, the lowest known E_{iso} overall. GRB 221009A is the record holder.

Table 3
The Highest Peak Flux GRBs from Our Input Samples, Selecting Some Bursts with the Highest Values in Each Instrument Sample

GRB Name	Interval (s) (s)	Peak Flux (erg s^{-1} cm^{-2})	Instrument	Reference
GRB 221009A	1.024	0.031	Konus, GBM	Frederiks et al. (2023), S. Lesage et al. (2023, in preparation)
GRB 140219A	0.064	1.22×10^{-3}	Konus	This work
GRB 110918A	0.064	9.02×10^{-4}	Konus	Frederiks et al. (2013), Tsvetkova et al. (2017)
GRB 920212	0.25	7.36×10^{-4}	PVO	Fenimore et al. (2023)
GRB 130427A	0.064	6.81×10^{-4}	Konus, GBM	Tsvetkova et al. (2017), Poolakkil et al. (2021)
GRB 230307A	1.024	6.71×10^{-4}	GBM, Konus	Dalessi et al. (2023), Svinkin et al. (2023)
GRB 830801	1	$\gtrsim 6.67 \times 10^{-4}$	SIGNE 2 MP9	Inferred from Kuznetsov et al. (1987)
GRB 900808	0.25	5.67×10^{-4}	PVO	Fenimore et al. (2023)
GRB 890923	0.25	5.54×10^{-4}	PVO	Fenimore et al. (2023)
GRB 811016	0.25	4.81×10^{-4}	PVO	Fenimore et al. (2023)
GRB 911226	0.25	4.73×10^{-4}	PVO	Fenimore et al. (2023)
GRB 021206	0.064	4.50×10^{-4}	Konus	This work
GRB 160625B	1.024	2.13×10^{-4}	GBM, Konus	Poolakkil et al. (2021), Tsvetkova et al. (2017)
GRB 131014A	1.024	1.57×10^{-4}	GBM, Konus	Tsvetkova et al. (2017), Poolakkil et al. (2021)
GRB 910402	1.62	1.47×10^{-4}	PHEBUS-GRANAT, BATSE	Barat et al. (1998)
GRB 940703	7.64	1.37×10^{-4}	PHEBUS-GRANAT, BATSE	Barat et al. (1998)
GRB 171227A	1.024	1.26×10^{-4}	GBM, Konus	This work
GRB 160821A	1.024	1.25×10^{-4}	GBM, Konus	Tsvetkova et al. (2017), Poolakkil et al. (2021)

Note. GRB 940703A and GRB 910402 were identified by BATSE, but we use the higher PHEBUS-GRANAT values for the same bursts. As no peak flux is reported for GRB 830801, we estimate a lower limit from Kuznetsov et al. (1987), noting that most of the energy flux occurs within a ~3 s interval, peaked at T0+0.5 to T0 +1.5 s. No claimed peak flux is within an order of magnitude of GRB 221009A.

but may arise, as the cataloged peak flux values are in photons, not ergs, which differs from the rest of our input samples. This issue does not affect our conclusions: GRB 221009A is again an obvious outlier with no burst within an order of magnitude. The brightest individual peak flux bursts are reported in Table 3.

3.3. Total Intrinsic Energy

GRB 221009A is obviously the BOAT as measured by prompt gamma-ray fluence, but the nearby distance and instrumental issues in the large GRB monitors due to burst brightness leave the question of how the total intrinsic energy,

Table 4
GRBs with $E_{\rm iso} > 2.5 \times 10^{54}$ erg

GRB Name	Redshift	Duration (s)	$E_{\rm iso}$ (erg)	Instrument	Reference
GRB 221009A	0.151	600	$\sim 1.2 \times 10^{55}$	Konus, GBM	Frederiks et al. (2023), S. Lesage et al. (2023, in preparation)
GRB 090323	3.6	130	5.81×10^{54}	Konus, GBM	Tsvetkova et al. (2017)
GRB 160625B	1.406	680	5.50×10^{54}	GBM, Konus	Abbott et al. (2017), Tsvetkova et al. (2017)
GRB 080916C	4.35	63	4.82×10^{54}	Konus, GBM	Abbott et al. (2017), Tsvetkova et al. (2017)
GRB 210619B	1.937	52	4.41×10^{54}	Konus	This work
GRB 130505A	2.27	32	4.37×10^{54}	Konus	Tsvetkova et al. (2017)
GRB 180914B	1.096	150	4.03×10^{54}	Konus	This work
GRB 170214A	2.53	150	3.94×10^{54}	Konus	This work
GRB 130907A	1.238	210	3.82×10^{54}	Konus	Tsvetkova et al. (2017)
GRB 220101A	4.618	240	3.64×10^{54}	Konus, GBM	This work
GRB 120624B	2.1974	270	3.45×10^{54}	GBM, Konus	Abbott et al. (2017), Tsvetkova et al. (2017)
GRB 090902B	1.822	19	3.26×10^{54}	GBM	Abbott et al. (2017)
GRB 170405A	3.51	80	2.89×10^{54}	Konus, GBM	This work, Abbott et al. (2017)
GRB 990123	1.6004	110	2.78×10^{54}	Konus, BATSE	Tsvetkova et al. (2017)
GRB 110918A	0.984	95	2.69×10^{54}	Konus	Tsvetkova et al. (2017)

Note. Bursts prior to the launch of Swift were included, but only GRB 990123 meets our threshold. GRB 221009A is the highest by nearly a factor of 2. Durations here are not a uniformly measured quantity (estimated from light curve, T_{90}, T_{100}) and are only intended to be approximate.

Table 5
GRBs with $L_{\rm iso} > 5 \times 10^{53}$ erg s^{-1}

GRB Name	Redshift	$L_{\rm iso}$ (erg s^{-1})	Instrument	Reference
GRB 110918A	0.984	2.70×10^{54}	Konus	Tsvetkova et al. (2017)
GRB 210619B	1.937	2.53×10^{54}	Konus, GBM	This work
GRB 221009A	0.151	$\sim 2.1 \times 10^{54}$	Konus, GBM	Frederiks et al. (2023), S. Lesage et al. (2023, in preparation)
GRB 160625B	1.406	2.04×10^{54}	GBM, Konus	Abbott et al. (2017), Tsvetkova et al. (2017)
GRB 130505A	2.27	1.91×10^{54}	Konus	Tsvetkova et al. (2017)
GRB 080916C	4.35	1.20×10^{54}	Konus, GBM	Abbott et al. (2017), Tsvetkova et al. (2017)
GRB 080607	3.0363	1.03×10^{54}	Konus	Tsvetkova et al. (2017)
GRB 130518A	2.488	9.67×10^{53}	GBM, Konus	Abbott et al. (2017), Tsvetkova et al. (2017)
GRB 090926A	2.1062	8.58×10^{53}	GBM, Konus	Abbott et al. (2017), Tsvetkova et al. (2017)
GRB 090902B	1.822	8.54×10^{53}	GBM	Abbott et al. (2017)
GRB 060121	4.6	7.58×10^{53}	Konus	Tsvetkova et al. (2017)
GRB 080721	2.591	7.05×10^{53}	Konus	Tsvetkova et al. (2017)
GRB 200829A	1.25	6.06×10^{53}	Konus, GBM	This work
GRB 220101A	4.618	5.27×10^{53}	Konus, GBM	This work
GRB 150403A	2.06	5.18×10^{53}	GBM, Konus	Abbott et al. (2017), Tsvetkova et al. (2017)
GRB 000131	4.5	5.01×10^{53}	Konus	Tsvetkova et al. (2017)

Note. Bursts prior to the launch of Swift were included, but only GRB 000131 meets our threshold. GRB 221009A is the third highest identified.

$E_{\rm iso}$, compares to the broader sample. Of the ∼400 GRBs with measured intrinsic energetics, those in Abbott et al. (2017), Tsvetkova et al. (2017), and Tsvetkova et al. (2021), as well as additional bursts compiled here, GRB 221009A is also the $E_{\rm iso}$ record holder. The Konus-Wind measurement is $\sim 1.2 \times 10^{55}$ erg, while the Fermi-GBM measurement is $\sim 1.0 \times 10^{55}$ erg, and An et al. (2023) even derive $\sim 1.5 \times 10^{55}$ erg from INSIGHT-HXMT and GECAM-C data. We have compiled a large $E_{\rm iso}$ sample, focusing on those with the highest measured values, shown in Figure 3. The closest bursts are only ∼50% of the value of GRB 221009A, as shown in Table 4.

3.4. Peak Isotropic-equivalent Luminosity

The peak luminosity of GRB 221009A is measured by Konus-Wind to be $\sim 2.1 \times 10^{54}$ erg s^{-1} (Frederiks et al. 2023) and by Fermi-GBM to be $\sim 1.0 \times 10^{54}$ erg s^{-1} over the 1.024 s interval. The other $L_{\rm iso}$ values we compare with are taken over the 1.024 s peak interval. For GBM-detected GRBs this is the reported value; for others we scale the reported value as described in Appendix B. GRB 221009A has an extreme but not record $L_{\rm iso}$, being at the ∼99th percentile of GRBs. The highest $L_{\rm iso}$ bursts are reported in Table 5, and the broader sample is shown in Figure 4.

4. Discussion

GRB 221009A is exceptional. It is, by far, the highest fluence and peak flux burst ever identified at Earth. It is additionally the record holder of $E_{\rm iso}$. It is also one of the highest $L_{\rm iso}$ bursts ever identified, though a few are known to be more luminous. These conclusions were independently made by both the Konus Team (Frederiks et al. 2023) and the GBM Team (S. Lesage et al. 2023, in preparation), and we refer the reader to their respective papers for these conclusions and detailed properties of the burst itself. In what follows, we explore the conclusions that can be drawn by comparing

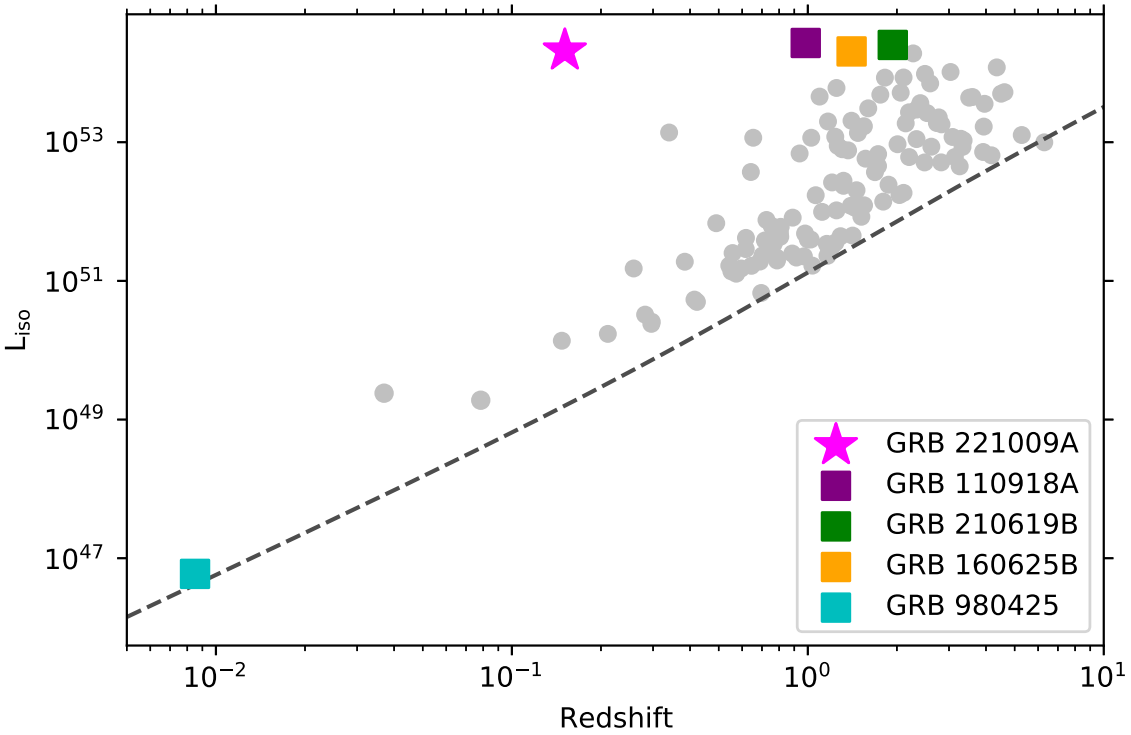

Figure 4. Bolometric, *k*-corrected L_{iso} for nearly 100 GRBs compiled from the literature (Abbott et al. 2017; Tsvetkova et al. 2017), with additional bright GRBs compiled following those works. The dashed line is an approximate, empirical detection threshold for GRBs as a function of redshift. Extreme GRBs are highlighted: GRB 110918A and GRB 210619B have higher L_{iso} than GRB 221009A. GRB 160625B is marked, as it is an analog of GRB 221009A, discussed in Section 4.6. We also show GRB 980425, as measured by BATSE, as one of the lowest known L_{iso} values in a GRB. GRB 221009A is *not* the record holder.

GRB 221009A with the total sample of the brightest GRBs identified thus far.

4.1. Rarity

GRB 221009A is out of class by both fluence and peak flux by around two orders of magnitude (when accounting for different peak flux intervals). Our fluence sample is largely complete for the observed sample. We are certain that no GRB with higher fluence than GRB 221009A exists in the observed sample, as it rivals even Galactic magnetar giant flares (Mazets et al. 1999; Palmer et al. 2005; Frederiks et al. 2007). The peak flux distribution is reasonably complete, though to a lesser extent than the fluence sample. However, any burst brighter than GRB 221009A in the 55 yr of observations would certainly have been noted, even if it occurred during intervals without publicly accessible data.

The brightest portions of both the fluence and peak flux cumulative distributions are expected to follow a $-3/2$ power law (e.g., Meszaros & Meszaros 1995). GRBs are detected beyond the regime of local structure; thus, for a GRB of a fixed intrinsic brightness distributed in a sensitive volume the recovered signals will have a cubic power corresponding to the spatial volume and a square root power for the inverse square law of intrinsic to observed brightness. This holds for distances sufficiently close to be approximated as Euclidean; for an expanding universe, the lower fluence or peak flux cumulative functions will be shallower (due to the additional $(1 + z)$ term for luminosity vs. comoving distance). This also holds only on the scale where source evolution is negligible. Both are true at the distance of GRB 221009A. The $-3/2$ scaling has been observationally confirmed for the high-fluence part of the log$N$–log$S$ and log$N$–log$P$ distributions (Mazets et al. 1981; Meegan et al. 1992; Fenimore et al. 1993a; von Kienlin et al. 2020). The shallower index for faint bursts (Meegan et al. 1992), combined with their isotropic distribution, is how the cosmological origin of GRBs was inferred (Briggs et al. 1996).

The most robust bright sample available is our combined, bolometric log$N$–log$S$ distribution constructed from bursts reported by Vela, PVO, BATSE, Konus-Wind, and Fermi-GBM (neglecting bursts seen only in other instruments), which has a value of 44.3 for effective 4π yr coverage. Assuming a $-3/2$ power-law index and fitting the scale directly to the median fluence values for bursts above 3×10^{-4} erg s^{-1} cm^{-2}, where our sample should be largely complete, gives a cumulative distribution function annual rate of GRBs above a given fluence S as $R_{GRB}(S) = 9.967 \times 10^{-6} \times S^{-3/2}$. The inverse of this rate gives a recurrence timescale as a function of fluence, i.e., $\tau(S) = 1.003 \times 10^{5} \times S^{+3/2}$. The bolometric fluence of GRB 221009A of 0.2 erg cm^{-2} has a recurrence rate at Earth of 9700 yr.

We can repeat this measurement while accounting for the uncertainty on the fluence of GRB 221009A and on the bursts used in the fit, either directly or by sampling the scaling distributions in Appendix A. Accounting for these uncertainties, a fit to the log$N$–log$S$ distribution with a fixed $-3/2$ index gives a recurrence time of 9200 yr and an uncertainty range of 7200–11,200 yr. Uncertainties in this paragraph are reported for the 80% confidence interval (i.e., 90% lower and 90% upper bounds). Allowing both scale and index to vary gives the measured index reported in Figure 1, confirming that we are in the regime where $-3/2$ power law is valid, and a corresponding median recurrence rate of 7400 yr and range of 3300–16,400 yr.

It is difficult to estimate this number by a combined log$N$–log$P$ given the different peak interval timescales. We measure it, neglecting errors, by scaling the 1.024 s peak flux of GRB 221009A to the peak flux intervals of the individual instrument distributions according to the procedure described in Appendix B. The values from Konus, GBM, and BATSE span 11,300–15,500 yr, suggesting that the peak flux recurrence rate is even more extreme. The individual instrument fluence recurrence rates (including PVO and Vela) span 6100–9600 yr. No matter how the recurrence rate is measured, its brightness at Earth occurs on the order of one time every ∼10,000 yr.

This value is substantially rarer than previous reports in the literature. The first reported rarity calculation in Atteia (2022) placed the recurrence rate at roughly every 500 yr, which helped motivate the original BOAT claims. Malesani et al. (2023) and O'Connor et al. (2023) perform a calculation similar to our method with claimed recurrence rates of 22–122 yr and 300–1100 yr, respectively. In these three cases our more stringent claim is largely driven by our use of the proper fluence value after accounting for instrumental effects, as the recurrence rates are a very strong function of brightness. Williams et al. (2023) utilize the collapsar evolution model from Lien et al. (2014) to place a lower limit of ∼1000 yr on the recurrence rate. Their use of a proper fluence value may suggest that GRB 221009A is unique compared to the broader modeled population, though we note that their lower limit is consistent with our measure.

While GRB 221009A is truly unique by observed brightness at Earth, it may not be unique by intrinsic brightness measures in the full observed prompt sample. There are more than 10,000 observed prompt GRBs, with only ∼1000 well localized (∼few arcminutes), but fewer than 500 bursts have determined isotropic-equivalent energetics values. In these 500, there are ∼20 bursts with an $E_{\rm iso}$ within a factor of 5 of GRB 221009A and ∼3 bursts within a factor of 2. As the observed prompt sample is 20 times larger, it is likely that there are bursts in the observed sample with $E_{\rm iso}$ greater than GRB 221009A but whose redshift or broadband spectra were not measured. There are two known GRBs with higher $L_{\rm iso}$ than GRB 221009A, and we similarly expect more to remain unidentified in the broader sample.

4.2. Why GRB 221009A Is the BOAT

GRB 221009A is certainly the BOAT at Earth. This is easily explained as being an intrinsically bright burst in unusual proximity to Earth. This requires only a particularly rare event. GRB 221009A was identified in a surprisingly small comoving volume, being 100 times smaller than the volume within which comparable bursts have been identified and 1000 times smaller than the volume it would have been detected within; this oddity is exacerbated when accounting for the declining source rates of collapsars since redshift ∼3 (Lien et al. 2014). Further, it is extremely surprising that this burst is also the prompt $E_{\rm iso}$ record holder. One possible observational bias is that much of the emission of the burst would not be recovered at Earth if GRB 221009A occurred at $z \approx 1$ or greater. However, the main emission episode is detectable deep into the universe and alone contains enough energy to be the record $E_{\rm iso}$.

The rarity of the event is not an explanation for why GRB 221009A is the $E_{\rm iso}$ record holder. One part of the explanation is the unusually high bulk Lorentz factor in this burst, either inferred through pair opacity arguments or requiring the GBM emission to be optically thin (S. Lesage et al. 2023, in preparation). In contrast to the prompt $L_{\rm iso}$ being near the record, the afterglow luminosity across the electromagnetic spectrum is within the observed distributions (Kann et al. 2023; Laskar et al. 2023; Williams et al. 2023). An unusually narrow jet opening angle could produce an intrinsically bright prompt signature while resulting in a more typical total kinetic energy in the jet. For GRB 221009A to match the highest collimation-corrected total energetics in the Konus sample (Tsvetkova et al. 2017, 2021), a collimation correction factor of ∼1000 is required, corresponding to a top-hat jet half-opening angle constraint of $<2\overset{\circ}{.}6$.

Making the strong assumption that the collimation-corrected prompt energetics of GRB 221009A are not in excess of the known collapsar class distributions, these observations allow us to understand what could have occurred to produce this burst. Due to unusual conditions either in jet formation and propagation or in the progenitor star and circumburst properties, the jet core achieved particularly high velocity while remaining very tightly collimated. This collimation was maintained despite a long-lived accretion phase, over 10 orders of magnitude in size from escape at the surface of the star to the external shock radius. This concentrated, highly energetic jet core was ideally aligned toward Earth.

Thus, either GRB 221009A has a concentrated, particularly energetic jet core, or GRB 221009A must also hold the collimation-corrected prompt energetics record, which would be all the more exceptional. A reasonably modeled jet structure and opening angle will give temporal and spectral index closure relations that are well matched by observations across the electromagnetic spectrum, providing a self-consistent check. The exceptional data set for this burst must contend with Galactic extinction due to alignment with the plane of the Milky Way, host galaxy extinction and contamination, and the expected supernova. Early results also utilize incomplete data sets. Below we place the prompt results in context with initial afterglow modeling of this burst, highlighting that a self-consistent picture has not emerged. Thus, a full understanding of why GRB 221009A is the (prompt) BOAT is not yet possible.

Williams et al. (2023) argue for a narrow jet using energetics arguments and report a steepening of the X-ray afterglow at 8×10^4 s, which would correspond to a half-jet opening angle of ∼2°. However, the observed temporal decay in X-rays is inconsistent with expectations for a top-hat jet. Laskar et al. (2023) include radio data and model the burst as occurring in a wind medium with a narrow jet opening angle of $\sim 1\overset{\circ}{.}5$. The corresponding kinetic energy $E_k \approx 4 \times 10^{50}$ erg, which is within the known distribution. They note the inability to fully match typical closure relations, and this model struggles to explain the lack of a jet break seen in optical light curves. A top-hat jet with opening angle of $1\overset{\circ}{.}5$ would give a collimation-corrected $E_\gamma \approx 4 \times 10^{51}$ erg, which is within the normal distributions (Tsvetkova et al. 2017, 2021). However, these E_k and E_γ values imply an unrealistic prompt gamma-ray efficiency of 90%.

A significantly narrower jet is disfavored with fiducial assumptions owing to upper limits on the afterglow polarization (Negro et al. 2023), though a narrower jet is possible if the typical assumed values for microphysical jet parameters are altered. Kann et al. (2023) note no jet break in the optical data

and infer a lower limit on the jet opening angle of $\sim 10^{\circ}$ (Kann et al. 2023). Assuming a top-hat jet with this value gives $E_{\gamma} \approx 2 \times 10^{53}$ erg, which would be substantially higher than any prior measured value (Cenko et al. 2011; Tsvetkova et al. 2017).

For previous particularly bright bursts, some have argued for a two-component jet model with a narrower ultrarelativistic jet surrounded by a wider jet with lower energy (e.g., Berger et al. 2003; Sheth et al. 2003; Racusin et al. 2008; Kann et al. 2018). Such a model may explain the nominally conflicting results reported and has been invoked for GRB 221009A (Sato et al. 2022). O'Connor et al. (2023) invoke a multicomponent jet model with an angular energy density dependence, declining as a broken power law. This broadly explains the afterglow data but would still require a record E_K and E_{γ}.

The picture is further complicated by potential contamination by the expected supernova signal. Fulton et al. (2023) assume that the optical emission and X-ray emission have no synchrotron break between them and model the differing temporal decays as arising from the emergence of the supernova. Shrestha et al. (2023) argue that a supernova cannot explain the temporal decay differences between these wavelengths and argue for no bright supernova. Levan et al. (2023) find the JWST spectra at $\sim$2 weeks after the prompt emission to be consistent with a power law, again arguing against a bright supernova. They model the afterglow with an early jet break (and thus a narrow jet) and with a spectral break between optical and X-rays, which differs from other analyses.

4.3. GRB 221009A at Greater Distances

For comparison of GRB 221009A to other bright GRBs, it is useful to consider how it would appear at greater redshifts more typical of the observed collapsar sample. In Figure 3 a dashed line is overlaid providing an approximate trigger threshold for Fermi-GBM, assuming that cosmological redshift effects on duration and observed energy are effectively counteracted by "tip-of-the-iceberg" effects from recovering only the bright, hard peaks of more distant bursts (Kocevski & Petrosian 2013; Moss et al. 2022). It is visually evident that this assumption is reasonable. The GRB 221009A prompt emission is composed of a triggering pulse, the main emission, and the last bright pulse at $\approx$T0+500 s. The initial pulse would trigger Fermi-GBM to $z \approx 1.3$ (S. Lesage et al. 2023, in preparation), beyond which it would trigger at the onset of the main pulse. The main emission would still be recovered beyond the highest redshift measured for any long GRB.

4.4. Implications for High-redshift GRBs

High-redshift GRBs, particularly those above $z \sim 6$, could be used to study early evolution of galaxies, to probe reionization, and to study metallicity from the death of the first stars (Tanvir et al. 2021). GRB 221009A could have been detected well beyond $z \sim 10$. At these distances the observed trigger would be on the pulse leading up to the brightest intervals, with a peak energy of $\sim$1–3 MeV (Frederiks et al. 2023; S. Lesage et al. 2023, in preparation). At a redshift of 10 this would be observed with an $E_{\rm peak}$ of 100–300 keV. Other GRBs detected beyond $z \approx 6$ show similar observed spectral hardness, e.g., the recent GRB 210905A at $z \sim 6.3$ and with peak energy of 145 keV (Rossi et al. 2022a). Thus, a population of GRBs with peak observed energies at Earth in the hundreds of keV should exist, which should be accounted for in the design of high-z GRB missions (Amati et al. 2021; White et al. 2021).

4.5. Comparison with Ultralong GRBs

Ultralong GRBs may be the longest-duration events belonging to the extreme tail of the long GRB sample, or they may be a distinct class with longer-lived central engines than typical collapsars. The threshold for inclusion in the ultralong class is not agreed on; we here explore thresholds of 1000 and 3600 s. Beyond $z \approx 0.7$ GRB 221009A would generally have an inferred duration beyond 1000 s owing to cosmological time dilation. For GRB 221009A to have a measured burst duration of longer than 3600 s (Kann et al. 2018) it would need to be beyond $z \approx 8.6$. For collapsars with measured redshift $\sim$75% are beyond $z \approx 0.7$ while few are beyond $z \approx 8.6$. GRB 221009A may or may not be a member of the putative ultralong GRB sample, depending on the threshold value assumed.

The Konus-Wind ultralong GRB sample (D. Svinkin, in preparation) is the most complete of any instrument, with nearly two dozen events beyond a 1000 s threshold. The highest fluence values of these bursts are $\sim(5\text{–}6) \times 10^{-4}$ erg cm^{-2} for GRB 080407 and the record-duration burst GRB 111209A. Thus, none of the Konus-Wind ultralong GRBs are remotely as bright as GRB 221009A. The highest peak flux values reach only $\sim 1 \times 10^{-5}$ erg s^{-1} cm^{-2} for GRB 080407 and GRB 961029. The typical ratio of peak flux to fluence for Konus ultralong GRBs is $\sim$3%, while GRB 221009A crosses the 10% boundary. This may suggest GRB 221009A as intermediate between typical long and ultralong GRBs, providing some support for a single continuum. There are additional GRBs that may fall into a similar range, including GRB 840304 (discussed next) and GRB 210905A with a duration of 870 s at a redshift of $z = 6.3$ (Rossi et al. 2022a).

4.6. Analogs

With the deep search of prompt GRB detections a few analogs to GRB 221009A have been identified. A close analog is GRB 990123. This burst is in the top 15 highest $E_{\rm iso}$ (Table 4), the $L_{\rm iso}$ is $(3\text{–}5) \times 10^{53}$ erg s^{-1}, the kinetic energy ($(1-5) \times 10^{50}$ erg) is comparable to the narrow-jet one for GRB 221009A (Laskar et al. 2023), and the half-jet opening angle is an unusually narrow $\sim 2^{\circ}$ (Zeh et al. 2006; Laskar et al. 2013; Tsvetkova et al. 2017). The burst occurs at $z = 1.604$ (Hjorth et al. 1999; Kelson et al. 1999), where the precursor pulse for GRB 221009A would not be recovered by GBM. More speculatively, the light curve resembles the onset of the main emission episode of GRB 221009A (Briggs et al. 1999).

GRB 160625B is perhaps the strongest analog when considering the full light curve: both have a weaker triggering pulse, quiescence for $\sim$175 s where the main emission occurs, with additional variable emission at $\sim$600 s. GRB 160625B occurred at a redshift of $z = 1.406$ (Xu et al. 2016) and has a comparable $L_{\rm iso}$. Both triggering pulses have particularly soft indices, but the spectral curvature occurs more than an order of magnitude lower in GRB 160625B compared to GRB 221009A (Zhang et al. 2018; Frederiks et al. 2023; S. Lesage et al. 2023, in preparation), while the GRB 160625B pulse has a far higher luminosity.

The only ultralong analog is GRB 840304, which is a top 5 burst by fluence, average burst by peak flux, and more than 1000 s long with two bright pulses followed by smooth

emission (Klebesadel et al. 1984). This profile sounds similar to GRB 221009A and may include afterglow in the duration calculation. Work is ongoing to find these data.

5. Conclusion

Prompt observations of GRB 221009A allow for a number of advancements in our understanding of these extreme events. We have here studied what can be learned from a comparison against the full detected prompt GRB sample, including strengthening some results already understood in Frederiks et al. (2023) and S. Lesage et al. (2023, in preparation).

Our results are summarized as follows:

1. GRB 221009A is the BOAT by three of the four measures of brightness. It is certainly the highest fluence and peak flux GRB ever identified, by a large margin. It is the highest $E_{\rm iso}$ burst ever identified and at the 99th percentile of $L_{\rm iso}$. These intrinsic extremes cannot be explained by observational bias.
2. While we have not directly measured higher $E_{\rm iso}$ in a GRB, it is likely that some of the prompt GRB detections, without known redshift or broadband spectra, have total energetics that exceed this burst.
3. We additionally explored the observation of this GRB had it occurred at greater distances, with implications for both ultralong GRBs and high-redshift GRBs.
4. We have here explored why GRB 221009A is so bright in the prompt emission, contributing to the advancement of understanding of this event. We identify three potential analogs whose joint study may prove fruitful.
5. We are unlikely to observe another event of such extreme brightness at Earth given the recurrence time on the scale of 10,000 yr. There is a reasonable chance this is the brightest burst at Earth since civilization began. If this rate calculation is correct, there is likely no brighter GRB signal within thousands of light-years. At any given time, only a few dozen such plane waves of intense radiation of similar or even higher intensity are traversing though the Milky Way.

We acknowledge the universe for timing this burst to arrive at Earth after the invention of GRB monitors but during our active research careers. Our token optical astronomer would like to complain about the alignment with the Galactic plane and requests that the next one avoid this issue. The paper is dedicated to all the unsung publications that make population analyses like this work possible, particularly those that we missed.

This paper is additionally dedicated to D. Alexander Kann, who unexpectedly passed away during the review of this paper. The above acknowledgments are left unchanged, as they were his suggestions. His expertise and input were key to this paper and many others. It is a small consolation to add this dedication to a paper that may be read in several thousand years, when the fluence record is broken. Alex will be sorely missed.

We thank Eve Chase and Chris Fryer for putting some key authors in contact, allowing for the largely complete data set. We thank the referee for prompt and valuable input.

J.F.A.F. acknowledges support from the Spanish Ministerio de Ciencia, Innovación y Universidades through grant PRE2018-086507. D.A.K. acknowledges the support by the State of Hessen within the Research Cluster ELEMENTS (Project ID 500/10.006).

R.H. acknowledges funding from the European Union's Horizon 2020 research and innovation program under the Marie Skodowska-Curie grant agreement No. 945298-ParisRegionFP.

Appendix A
Fluence and Peak Flux Bolometric Scalings

A major analysis portion of this paper is the conversion of reported fluence and peak flux values for GRB monitors that operated and reported in energy ranges narrower than the bolometric range of interest here. Konus values are already sufficiently close to bolometric. For BATSE and GBM bursts where the best-fit spectral form constrains curvature we directly integrate the fit parameters over the bolometric energy range. For Vela, PVO, and BATSE and GBM bursts best fit by a power law (where extrapolation would overestimate the true bolometric values), we must apply a scaling distribution to convert from one energy range to another. These scaling distributions can be constructed by taking the scaling values for a large sample of GRBs with measured spectral curvature from one energy range to another. For this we use the GBM 10 Year Spectral Catalog (Poolakkil et al. 2021), which contains a complete spectral analysis to determine the best-fit spectrum over the full T_{90} interval and the peak flux interval, set to the 1.024 s timescale for long GRBs.

For the fluence sample there are 1938 bursts considered. Of these, 376 are best fit by a power law, and 1562 are best fit by a model with constrained curvature, i.e., a Comptonized function, Band, or a smoothly broken power law. The GBM fit is performed over the $\sim$8 keV−39 MeV energy range, meaning that this is a slight extrapolation on the low end but otherwise within the GBM bandpass. For these 1562 bursts we determine the scaling factor and uncertainty to convert between energy ranges on a burst-by-burst basis. These measures are constructed into a distribution, which gives the averaged scaling and uncertainties. For conversion of the GBM 10–1000 keV fluence to the bolometric band we get a scaling value of $1.28^{+1.11}_{-0.24}$, with the full distribution shown in Figure 5.

We can repeat the same procedure, except instead of converting the 10–1000 keV fluence to the bolometric, we convert it to the reported energy ranges for the other instruments, i.e., 300–1500 keV for Vela, 50–300 keV for PVO (utilizing the values reported in Fenimore et al. 2023), and 20–2000 keV for BATSE. For the Vela comparison we remove bursts with $E_{\rm peak} < 300$ keV, necessary to avoid overcorrection. The final scaling factors are the convolution of two of these distributions, i.e., for Vela the final values convolve the 10–1000 keV to bolometric energy range with the inverse of the 10–1000 keV to 300–1500 keV energy range, allowing for a mapping from the 300–1500 keV fluence to the bolometric range.

For the peak flux intervals, the same procedure can be applied, with the results shown in Figure 6. The peak flux scaling distributions are calculated based on the peak flux spectral fit parameter values in the GBM Spectral Catalog (Poolakkil et al. 2021). This is necessary given the generally harder spectra during peak flux intervals, as compared to the time-integrated fits, resulting in a slightly larger overall scaling value.

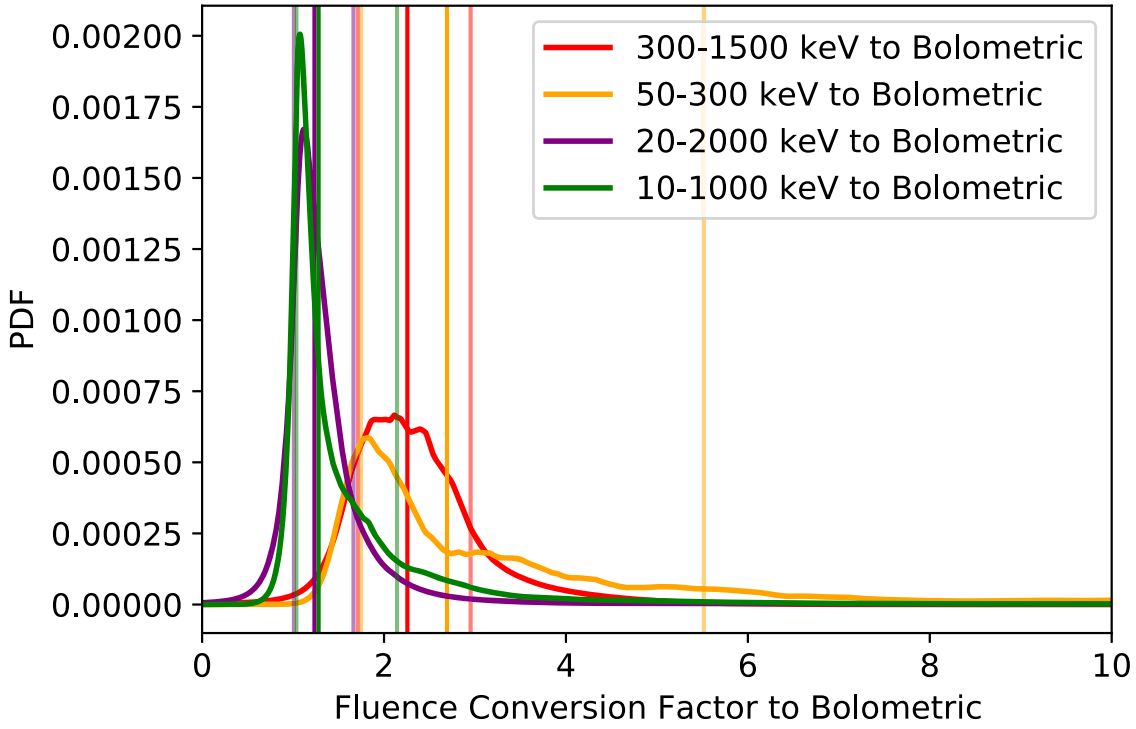

Figure 5. The probability density function of scaling fluence as measured in a given energy range to the 1 keV−10 MeV bolometric energy range.

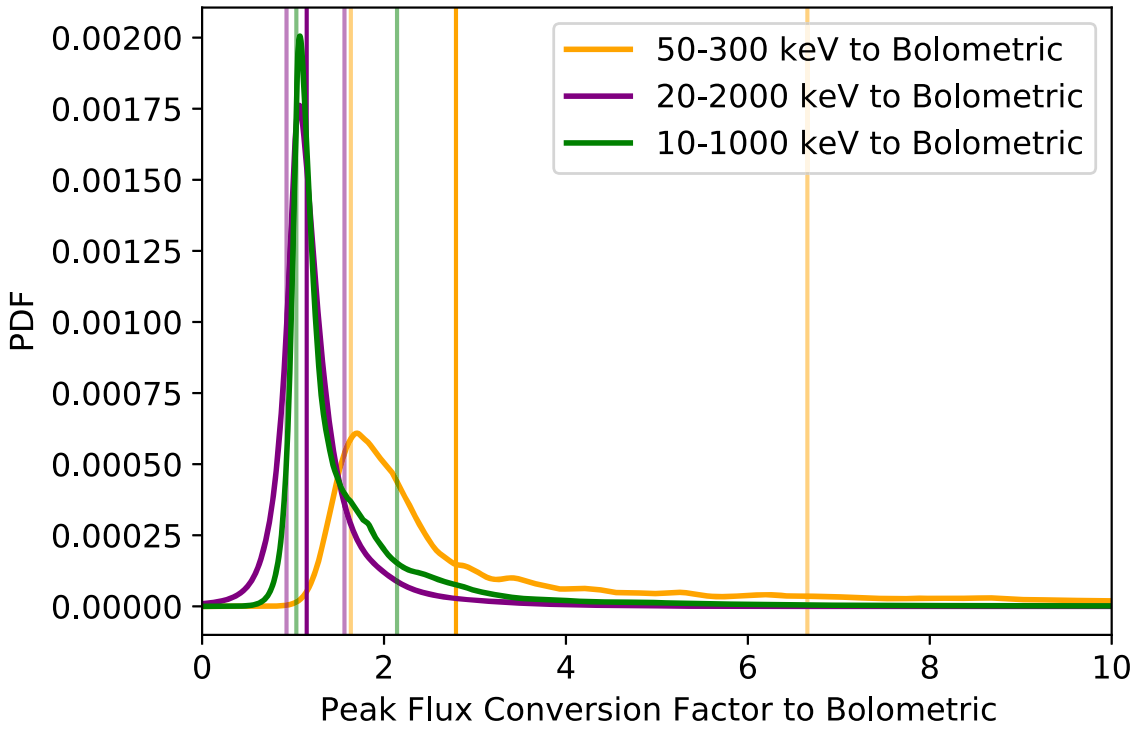

Figure 6. The probability density funtion of scaling peak flux as measured in a given energy range to the 1 keV−10 MeV bolometric energy range. Note the particularly significant skew in the PVO extrapolation (50–300 keV), which may explain our anomalous PVO peak flux values.

Appendix B
Peak Flux Interval Scalings

In order to compare peak flux values between instruments to identify the brightest individual bursts, we utilize parameters from the Fermi-GBM Ten Year Catalog (von Kienlin et al. 2020). The GBM calculation of duration is T_{90}, which is the time between the integrated 5% and 95% of the total burst fluence. This is determined by fitting time-resolved slices from pre-burst background to post-burst background, assuming a Comptonized function. An output of this analysis is a measure of the peak flux over 0.064, 0.256, and 1.024 s intervals.

From comparing the sample the 0.064 s peak flux is $1.31^{+0.22}_{-0.22}$ times the 0.256 s interval. The 0.256 s peak flux value is

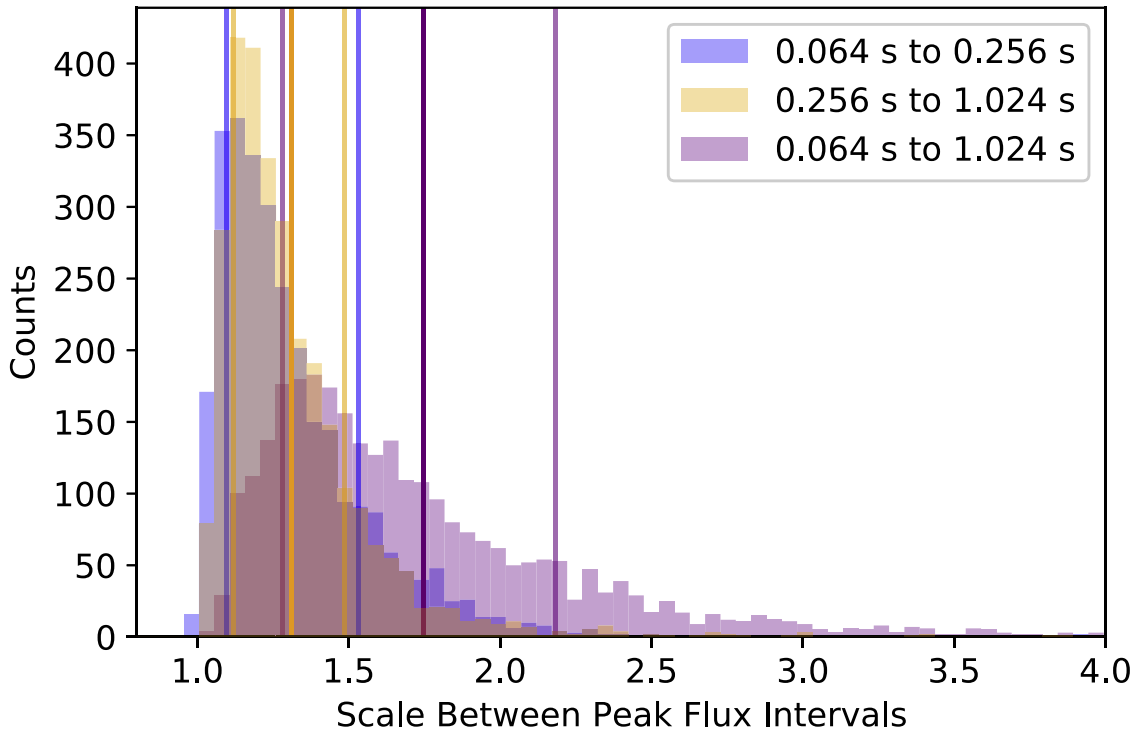

Figure 7. The distribution of the ratios of a given GBM peak flux interval against another. Vertical lines denote the median and 1σ bounds for each distribution. The 0.064–0.256 s and 0.256–1.024 s means are nearly identical and overlaid on the figure.

$1.31^{+0.18}_{-0.19}$ times the 1.024 s interval. Lastly, the 0.064 s is $1.75^{+0.44}_{-0.47}$ times the 1.024 s values. These are mean values with 1σ uncertainties. The full distributions are shown in Figure 7. Noting that $1.31^2 = 1.72$, we see that each factor of two in peak flux interval scales as $\sqrt{1.31} \approx 1.15$, or ∼15%. The scale invariance and reasonable error bars allow us to scale peak flux intervals from different instruments into a standardized range. While not valid on each individual burst, the population scalings are accurate. Individual variation will not affect our conclusions here, as no burst is close to GRB 221009A in peak flux and the $L_{\rm iso}$ measure is already bounded.

ORCID iDs

Eric Burns https://orcid.org/0000-0002-2942-3379
Dmitry Svinkin https://orcid.org/0000-0002-2208-2196
D. Alexander Kann https://orcid.org/0000-0003-2902-3583
José Feliciano Agüí Fernández https://orcid.org/0000-0001-6991-7616
Dmitry Frederiks https://orcid.org/0000-0002-1153-6340
Rachel Hamburg https://orcid.org/0000-0003-0761-6388
Stephen Lesage https://orcid.org/0000-0001-8058-9684
Yuri Temiraev https://orcid.org/0000-0003-4813-8378
Anastasia Tsvetkova https://orcid.org/0000-0003-0292-6221
Elisabetta Bissaldi https://orcid.org/0000-0001-9935-8106
Michael S. Briggs https://orcid.org/0000-0003-2105-7711
Sarah Dalessi https://orcid.org/0000-0003-1835-570X
Rachel Dunwoody https://orcid.org/0000-0003-3248-5447
Cori Fletcher https://orcid.org/0000-0002-0186-3313
Adam Goldstein https://orcid.org/0000-0002-0587-7042
C. Michelle Hui https://orcid.org/0000-0002-0468-6025
Boyan A. Hristov https://orcid.org/0000-0001-9556-7576
Daniel Kocevski https://orcid.org/0000-0001-9201-4706
Alexandra L. Lysenko https://orcid.org/0000-0002-3942-8341
Bagrat Mailyan https://orcid.org/0000-0002-2531-3703
Joseph Mangan https://orcid.org/0000-0002-6849-5009
Sheila McBreen https://orcid.org/0000-0002-1477-618X
Judith Racusin https://orcid.org/0000-0002-4744-9898
Anna Ridnaia https://orcid.org/0000-0001-9477-5437
Oliver J. Roberts https://orcid.org/0000-0002-7150-9061
Mikhail Ulanov https://orcid.org/0000-0002-0076-5228
Peter Veres https://orcid.org/0000-0002-2149-9846
Colleen A. Wilson-Hodge https://orcid.org/0000-0002-8585-0084
Joshua Wood https://orcid.org/0000-0001-9012-2463

References

Abbasi, R., Ackermann, M., Adams, J., et al. 2023, arXiv:2302.05459
Abbott, B. P., Abbott, R., Abbott, T. D., et al. 2017, ApJL, 848, L13
Agüí Fernández, J. F., Thöne, C. C., Kann, D. A., et al. 2023, MNRAS, 520, 613
Ahumada, T., Singer, L. P., Anand, S., et al. 2021, NatAs, 5, 917
Amati, L., O'Brien, P., Götz, D., et al. 2021, ExA, 52, 183
An, Z.-H., Antier, S., Bi, X.-Z., et al. 2023, arXiv:2303.01203
Aptekar, R. L., Frederiks, D. D., Golenetskii, S. V., et al. 1995, SSRv, 71, 265
Atteia, J. L. 2022, GCN, 32793, 1
Band, D., Matteson, J., Ford, L., et al. 1993, ApJ, 413, 281
Barat, C., Lestrade, J. P., Dezalay, J. P., et al. 1998, in AIP Conf. Ser. 428, Gamma-Ray Bursts, 4th Hunstville Symp., ed. C. A. Meegan, R. D. Preece, & T. M. Koshut (Melville, NY: AIP), 278
Barthelmy, S. D., Barbier, L. M., Cummings, J. R., et al. 2005, SSRv, 120, 143
Berger, E., Kulkarni, S. R., Pooley, G., et al. 2003, Natur, 426, 154
Bloom, J. S., Frail, D. A., & Sari, R. 2001, AJ, 121, 2879
Briggs, M., Band, D., Kippen, R., et al. 1999, ApJ, 524, 82
Briggs, M. S., Paciesas, W. S., Pendleton, G. N., et al. 1996, ApJ, 459, 40
Burns, E., Svinkin, D., Hurley, K., et al. 2021, ApJL, 907, L28
Burrows, D. N., Hill, J. E., Nousek, J. A., et al. 2005, SSRv, 120, 165
Cano, Z., Wang, S.-Q., Dai, Z.-G., & Wu, X.-F. 2017, AdAst, 2017, 8929054
Cenko, S. B., Frail, D. A., Harrison, F. A., et al. 2011, ApJ, 732, 29

Chuang, K.-W. 1990, PhD thesis, Univ. of California, Riverside
Dalessi, S., Roberts, O. J., & Meegan, C. 2023, GCN, 33411, 1
de Ugarte Postigo, A., Izzo, L., Pugliese, G., et al. 2022, GCN, 32648, 1
Dezalay, J.-P., Barat, C., Talon, R., et al. 1991, in AIP Conf. Proc. 265, Gamma-ray bursts, ed. W. Paciesas & G. J. Fishman (Melville, NY: AIP), 304
Fenimore, E., Epstein, R., Ho, C., et al. 1993a, Natur, 366, 40
Fenimore, E., Schwarz, G., Lamb, D. Q., Freeman, P., & Murakami, T. 1993b, in AIP Conf. Ser. 290, Compton Gamma-Ray Observatory, ed. M. Friedlander, N. Gehrels, & D. Macomb (New York: AIP), 917
Fenimore, E. E., Crider, A., int Zand, J. J. M., et al. 2023, arXiv:2302.12859
Frederiks, D., Golenetskii, S., Aptekar, R., et al. 2018, GCN, 23240, 1
Frederiks, D., Golenetskii, S., Palshin, V., et al. 2007, AstL, 33, 1
Frederiks, D., Lysenko, A., Ridnaia, A., et al. 2022, GCN, 32668, 1
Frederiks, D., Svinkin, D., Lysenko, A. L., et al. 2023, arXiv:2302.13383
Frederiks, D. D., Hurley, K., Svinkin, D. S., et al. 2013, ApJ, 779, 151
Fulton, M. D., Smartt, S. J., Rhodes, L., et al. 2023, arXiv:2301.11170
Galama, T. J., Vreeswijk, P., Van Paradijs, J., et al. 1998, Natur, 395, 670
Gehrels, N., Chincarini, G., Giommi, P., et al. 2004, ApJ, 611, 1005
Goldstein, A., Preece, R. D., Mallozzi, R. S., et al. 2013, ApJS, 208, 21
Goldstein, A., Veres, P., Burns, E., et al. 2017, ApJL, 848, L14
Golenetskii, S., Aptekar, R., Frederiks, D., et al. 2014, GCN, 15870, 1
Gompertz, B. P., Ravasio, M. E., Nicholl, M., et al. 2023, NatAs, 7, 67
Gotz, D., Mereghetti, S., Savchenko, V., et al. 2022, GCN, 32660, 1
Guidorzi, C., Lacapra, M., Frontera, F., et al. 2011, A&A, 526, A49
Hakkila, J., Pendleton, G. N., Meegan, C. A., et al. 2003, in AIP Conf. Ser. 662, Gamma-Ray Burst and Afterglow Astronomy 2001: A Workshop Celebrating the First Year of the HETE Mission, ed. G. R. Ricker & R. K. Vanderspek (Melville, NY: AIP), 176
Hjorth, J., Andersen, M. I., Cairos, L. M., et al. 1999, GCN, 219, 1
Huang, Y., Hu, S., Chen, S., et al. 2022, GCN, 32677, 1
Kann, D. A., Agayeva, S., Aivazyan, V., et al. 2023, arXiv:2302.06225
Kann, D. A., Schady, P., Olivares, E. F., et al. 2018, A&A, 617, A122
Kelson, D., Illingworth, G., Franx, M., Magee, D., & van Dokkum, P. 1999, IAUC, 7096, 3
Klebesadel, R., Evans, W., Glore, J., Spalding, R., & Wymer, F. 1980, ITGRS, 76, 1
Klebesadel, R., Laros, J., & Fenimore, E. 1984, BAAS, 16, 1016
Klebesadel, R. W., Strong, I. B., & Olson, R. A. 1973, ApJL, 182, L85
Kocevski, D., & Petrosian, V. 2013, ApJ, 765, 116
Kouveliotou, C., Meegan, C. A., Fishman, G. J., et al. 1993, ApJL, 413, L101
Kozlova, A., Golenetskii, S., Aptekar, R., et al. 2016, GCN, 19842, 1
Kozyrev, A. S., Golovin, D. V., Litvak, M. L., et al. 2022, GCN, 32805, 1
Kuznetsov, A., Sunyaev, R., Terekhov, O., et al. 1987, PAZh, 13, 1055
Lapshov, I., Molkov, S., Mereminsky, I., et al. 2022, GCN, 32663, 1
Laskar, T., Alexander, K. D., Margutti, R., et al. 2023, arXiv:2302.04388
Laskar, T., Berger, E., Tanvir, N., et al. 2013, ApJ, 781, 1
Levan, A. J., Lamb, G. P., Schneider, B., et al. 2023, arXiv:2302.07761
Lien, A., Sakamoto, T., Gehrels, N., et al. 2014, ApJ, 783, 24
Liu, J. C., Zhang, Y. Q., Xiong, S. L., et al. 2022, GCN, 32751, 1
Malesani, D. B., Levan, A. J., Izzo, L., et al. 2023, arXiv:2302.07891
Mazets, E. P., Aptekar, R. L., Cline, T. L., et al. 2008, ApJ, 680, 545
Mazets, E. P., Cline, T. L., Aptekar', R. L., et al. 1999, AstL, 25, 635
Mazets, E. P., Golenetskii, S. V., Ilinskii, V. N., et al. 1981, Ap&SS, 80, 3
Mazets, E. P., Golentskii, S. V., Ilinskii, V. N., Aptekar, R. L., & Guryan, I. A. 1979, Natur, 282, 587
Meegan, C., Fishman, G., Wilson, R., et al. 1992, Natur, 355, 143
Meszaros, P., & Meszaros, A. 1995, ApJ, 449, 9
Moss, M., Lien, A., Guiriec, S., Cenko, S. B., & Sakamoto, T. 2022, ApJ, 927, 157
Murase, K., Mukhopadhyay, M., Kheirandish, A., Kimura, S. S., & Fang, K. 2022, ApJL, 941, L10
Negro, M., Di Lalla, N., Omodei, N., et al. 2023, arXiv:2301.01798
O'Connor, B., Troja, E., Ryan, G., et al. 2023, arXiv:2302.07906
Palmer, D. M., Barthelmy, S., Gehrels, N., et al. 2005, Natur, 434, 1107
Piano, G., Verrecchia, F., Bulgarelli, A., et al. 2022, GCN, 32657, 1
Piran, T. 1999, PhR, 314, 575
Poolakkil, S., Preece, R., Fletcher, C., et al. 2021, ApJ, 913, 60
Racusin, J., Liang, E., Burrows, D. N., et al. 2009, ApJ, 698, 43
Racusin, J. L., Karpov, S., Sokolowski, M., et al. 2008, Natur, 455, 183
Rastinejad, J. C., Gompertz, B. P., Levan, A. J., et al. 2022, Natur, 612, 223
Ripa, J., Takahashi, H., Fukazawa, Y., et al. 2023, arXiv:2302.10047
Roming, P. W. A., Kennedy, T. E., Mason, K. O., et al. 2005, SSRv, 120, 95
Rossi, A., Frederiks, D. D., Kann, D. A., et al. 2022a, A&A, 665, A125
Rossi, A., Rothberg, B., Palazzi, E., et al. 2022b, ApJ, 932, 1
Sari, R., Piran, T., & Halpern, J. P. 1999, ApJL, 519, L17
Sato, Y., Murase, K., Ohira, Y., & Yamazaki, R. 2022, arXiv:2212.09266
Savchenko, V., Ferrigno, C., Kuulkers, E., et al. 2017, ApJL, 848, L15
Sheth, K., Frail, D. A., White, S., et al. 2003, ApJL, 595, L33
Shrestha, M., Sand, D. J., Alexander, K. D., et al. 2023, arXiv:2302.03829
Strong, I. B., Klebesadel, R. W., & Olson, R. A. 1974, ApJL, 188, L1
Svinkin, D., Frederiks, D., Hurley, K., et al. 2021, Natur, 589, 211
Svinkin, D., Frederiks, D., Ulanov, M., et al. 2023, GCN, 33427, 1
Tanvir, N. R., Le Floc'h, E., Christensen, L., et al. 2021, ExA, 52, 219
Tiengo, A., Pintore, F., Vaia, B., et al. 2023, arXiv:2302.11518
Troja, E., Fryer, C. L., O'Connor, B., et al. 2022, Natur, 612, 228
Tsvetkova, A., Frederiks, D., Golenetskii, S., et al. 2017, ApJ, 850, 161
Tsvetkova, A., Frederiks, D., Svinkin, D., et al. 2021, ApJ, 908, 83
Tsvetkova, A., Svinkin, D., Karpov, S., & Frederiks, D. 2022, Univ, 8, 373
Ursi, A., Panebianco, G., Pittori, C., et al. 2022, GCN, 32650, 1
Veres, P., Burns, E., Bissaldi, E., et al. 2022, GCN, 32636, 1
von Kienlin, A., Meegan, C. A., Paciesas, W. S., et al. 2020, ApJ, 893, 46
White, N. E., Bauer, F. E., Baumgartner, W., et al. 2021, Proc. SPIE, 11821, 1182109
Williams, M. A., Kennea, J. A., Dichiara, S., et al. 2023, arXiv:2302.03642
Xiao, H., Krucker, S., & Daniel, R. 2022, GCN, 32661, 1
Xu, D., Malesani, D., Fynbo, J. P. U., et al. 2016, GCN, 19600, 1
Zeh, A., Klose, S., & Kann, D. A. 2006, ApJ, 637, 889
Zhang, B. 2018, The Physics of Gamma-Ray Bursts (Cambridge: Cambridge Univ. Press)
Zhang, B. B., Liu, Z. K., Peng, Z. K., et al. 2021, NatAs, 5, 911
Zhang, B.-B., Zhang, B., Castro-Tirado, A. J., et al. 2018, NatAs, 2, 69